

Ordered Assembly of Pd Nanoparticles on Electronic Substrates

U. Pal^{1*}, and M. Herrera-Zaldívar²

¹*Instituto de Física, Universidad Autónoma de Puebla, Apdo. Postal J-48, Puebla, Pue. 72570, Mexico. E-mail: upal@sirio.ifuap.buap.mx*

²*Centro de Ciencias de la Materia Condensada, Universidad Nacional Autónoma de México, Apdo. Postal 2681, Ensenada, BC 22800, Mexico. E-mail: Zaldivar@ccmc.unam.mx*

PACS: 81.07.Bc, 81.16.Dn, 81.16.Rf, 81.20.Ka, 68.37.Ef

Abstract

Room temperature assembly of Pd nanoparticles on solid electronic substrates like Si, SiC and C are studied. A one-step chemical reduction method without any surfactant or functionalizing agent was used. The Pd nanoparticles of different average sizes could be nucleated and grown in well-organized manner over a large area of C and C-terminated SiC substrates, while the nanoparticles formed on Si or Si-terminated SiC substrates did not organize well. By controlling the process parameters, the average diameter of the Pd nanoparticles could be controlled. It is found that the unsaturated C bonds on the substrate surface play the main role for organizing Pd nanoparticles on them. The Pd nanoparticles on the solid substrates are well crystalline and retain their bulk crystal structure.

Short Title: Assembly of Pd nanoparticles

*Corresponding author, Fax: +52-222-2295611

1. Introduction

Controlled assembly of nanoparticles on solid substrates has been one of the most promising tools in Nanotechnology. Self-assembly based strategies are believed to have a major impact in the manufacturing of systems in the micro, and nanometer scale (1,2). Once a controlled self-assembly is achieved through manipulation at nanometer scale, components and devices could be fabricated exploiting the size-dependent properties of nanoparticles.

Several pathways have been developed in the last decade to create tailored nanoparticle assemblies utilizing different forces for different material. The acting forces, which might have different physical origins (3,4), must act over the scale comparable to the feature size, and therefore much longer ranging than atomic bond length (5). A broadly accepted technique is the so-called layer-by-layer (LBL) assembly utilizing polyelectrolytes as molecular glue between the substrate and nanoparticles or between successive nanoparticle layers (6,7). The technique is very popular for the assembly of nanoparticle layers on macroscopic surfaces, production of micropatterns (8) on mesoscopic (9) and microscopic substrates (10).

Very recently, Correa-Duarte and Liz-Marzán (11) used polyelectrolytes for wrapping carbon nanotubes and providing them absorption sites for electro-statically driven nanoparticle deposition. Most of the advances and efforts concerning the assembly of nanoclusters onto solid surfaces were driven by potential applications in catalysis (12), sensors (13-15), and nanoelectronics (16). Assembled metal and semiconductor nanoclusters provide interesting properties for these applications.

Though the earlier reports on the generation of metal-cluster assemblies were mostly restricted for silicon substrates (17-19), recently Vidoni et al (20) have described the elaboration of closed-packed arrangement of gold colloids on GaAs substrates through edification of a self-assembly monolayer of molecules. While the multilayer lamellar films of metal nanoclusters have been grown by LB technique (21,22) utilizing electrostatic-immobilization process and metal nanoparticles could be assembled on solid surfaces utilizing electrostatic interaction between the ionized amine group of solid support and carboxylic group of thiol (capping layer of nanoparticles) (23), recently we reported the use of ion-dipole interaction between the amine group and PVP (covered on Au-Pd nanoparticles) as a general and easy technique for the organization of metal clusters on any solid substrate (24). Even the assembly of metal clusters on the defect sites such as dislocations and grain

boundaries of solid electronic substrates has been studied for quite a long time [25-28], recent prospect of versatile applications of nanocluster assemblies generated a huge thrust for their uniform 2-D assemblies on solid substrates. In ex-situ processes, apart from the defect site induced assemblies, carboxylic acid, or amine groups are being used to produce self-assembled nanoparticles on solid substrates. Although, for catalytic and biological applications, use of such organic substances may not have any adverse effect on the performance of the assemblies, for electronic applications they are bound to affect device performance.

In the present study we tried to fabricate Pd nanocluster assemblies on several electronic substrates like C, SiC and Si without using any capping agent either on the metal clusters or on the substrates. By chemical reduction of the Pd ions in a methanolic solution in presence of solid electronic substrates, site selective assemblies of Pd nanoclusters could be fabricated over C-terminated SiC layers and amorphous C substrates. The nanoparticle assemblies were studied by SEM, EDS and STM techniques. Nucleation and growth of Pd clusters at the unsaturated c-sites are proposed as the mechanism for their assembled growth on the C-terminated SiC and amorphous C substrates.

2. Experimental

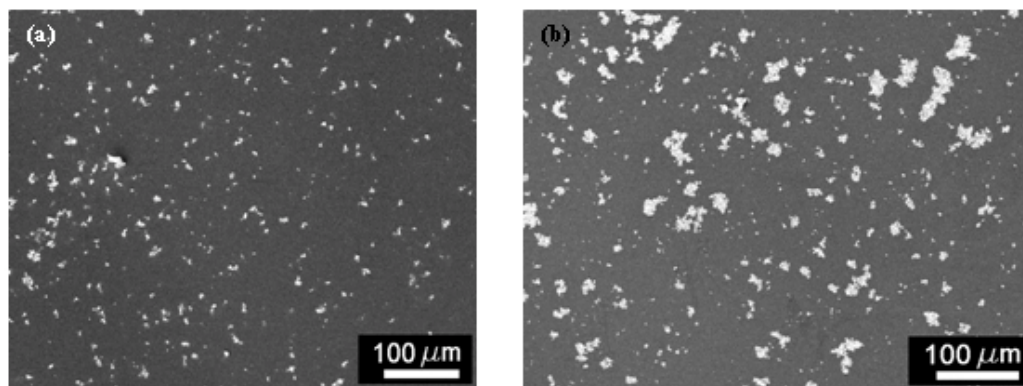
Pd nanoparticles on different substrates like SiC and carbon were grown by reducing the palladium metal ions on the substrate surfaces. In a typical synthesis process, either of the solid substrates such as SiC (6H) wafer (epitaxially grown, CREE H0124-15), SiC (4H) wafer (Epitaxially grown, CREE E0319-3), amorphous carbon (carbon coated microscopic grids, Nissin EM Co., LTD.) and Si (100) (Crysteco 1702-3) was immersed into 10 ml methanolic solution of PdCl₂ (Alfa Aesar, 99.9%; 0.033 mmol/50 ml of methanol) under mild agitation. Then about 0.5 ml of aqueous solution of NaBH₄ (0.044 M) was added to it drop-wise. After the addition of the reductor (NaBH₄ solution), the substrate was removed from the solution at different intervals of time. The substrates were then rinsed in methanol and dried in air at room temperature. Typical size of the SiC (6H), SiC (4H) and Si (100) wafers used as substrates was of about 5 mm x 5 mm, while the size of the C-coated copper grids was 3 mm diameter.

A JEOL JSM5300 scanning electron microscope (SEM), attached with a Thermo Noran Super-dry II energy dispersive X-ray spectrometer (EDS) was used for the

morphology and composition analysis of the samples. A NanoScope E STM (Digital Instruments) operated in ambient condition was employed for the topographic characterizations. All the STM images presented in this work were taken in constant current (topographical) mode, using electrochemically etched W wires as probe-tips. For scanning tunnelling spectroscopy (STS), mechanically sharpened Pt-Ir wires were used as tips. I-V data were collected following a common procedure: the feedback loop of the microscope that controls the vertical motion of the tip was interrupted momentarily and the bias voltage was digitally ramped from an initial to a final pre-selected value, while the corresponding tunnel current was digitally sampled.

3. Results and Discussion

Figure 1 shows the SEM images of the Pd clusters deposited over Si substrate at different times of immersion. We can observe the formation of nanoclusters over the substrate in unassembled manner. While for 5 min of immersion, the clusters remained well dispersed over the substrate, for longer time of immersion more clusters were formed and aggregated to form bigger clusters. Formation of Pd clusters on Si substrate in irregular manner indicates that the initial nucleations occurred at the defect sites such as dislocations of the substrate. On longer time of immersion, more Pd clusters are formed in the reaction solution and aggregated to the initial clusters on the substrate.



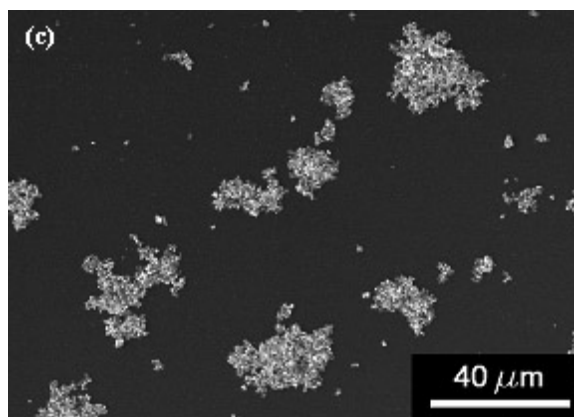


Figure 1 - Typical SEM images of Pd clusters deposited over Si substrate for a) 5 min, and b-c) 15 min of immersion in the reaction solution. The scale bars in a), b), and c) are 100, 100 and 40 μm respectively.

The formation pattern of Pd clusters on Si-terminated SiC (4H) substrate is quite similar to that of Si substrate. In figure 2, the SEM micrographs of the Pd cluster deposited Si-terminated SiC substrate are presented.

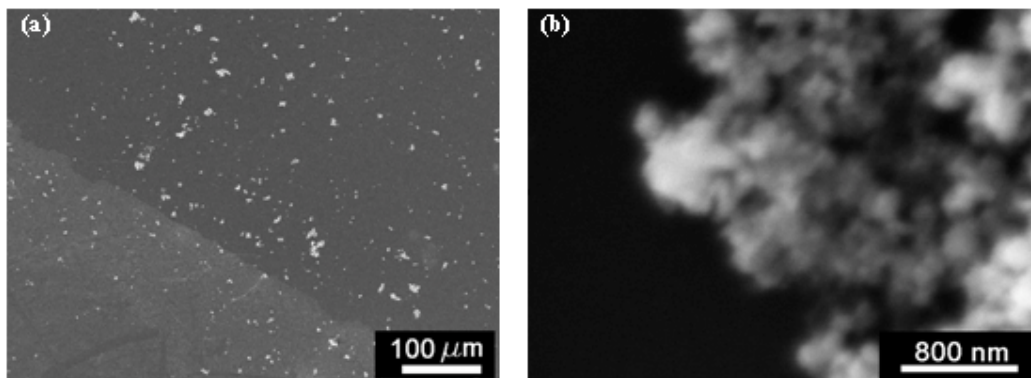


Figure 2 - Typical SEM images of Pd clusters deposited over Si-terminated SiC substrate for a) 5 min, and b) 15 min of immersions in the reaction solution. The scale bars in a) and b) are 100 μm and 800 nm respectively.

In figure 3, the formation of Pd clusters and their assemblies over the C-terminated SiC (6H) substrates are presented. From the SEM images, we can see that the Pd nanoclusters are formed all over the substrate surface with well arranged assemblies and regular size. The size of the Pd clusters increased slightly with the increase of immersion time of the substrate.

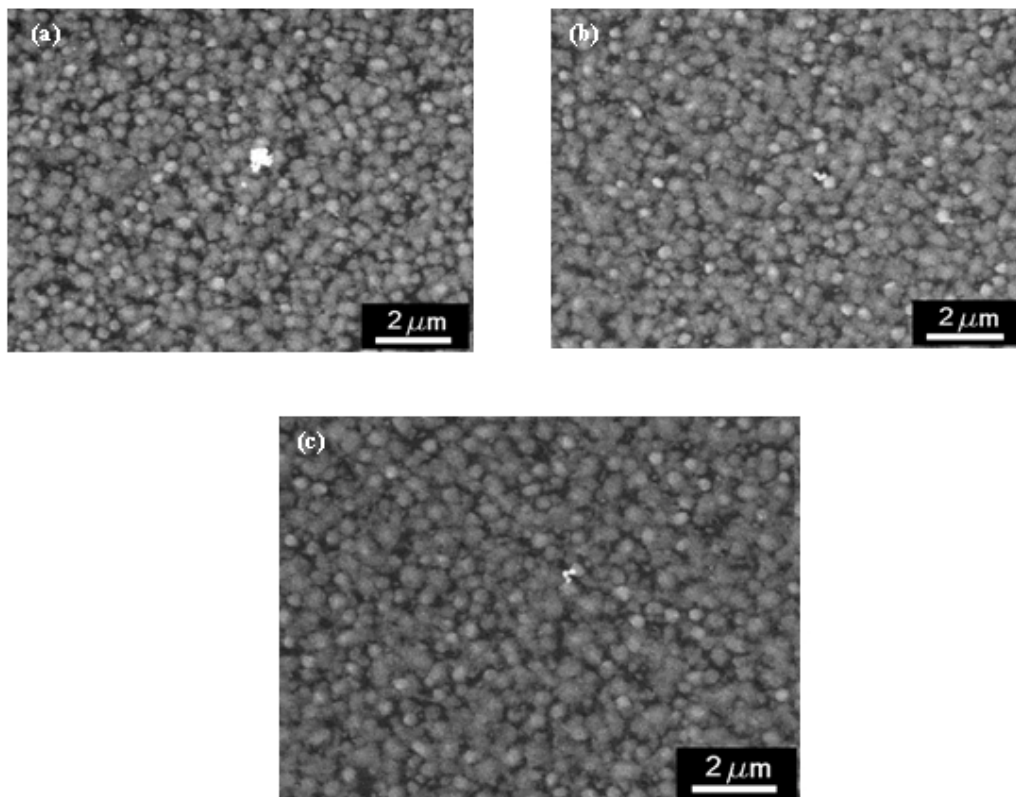


Figure 3 - Typical SEM images of the Pd clusters formed over C-terminated SiC substrate for a) 2 min, b) 5 min, and c) 20 min of immersions in the reaction solution.

The formation and assembly of Pd nanoclusters over C-coated Cu grids are shown in figure 4. With the increase of immersion time the clusters grown bigger, and for longer immersion times, some agglomerated structures are formed over the surface. It should be noted that the carbon coating over the microscopic grid was of amorphous nature. Formation of well-ordered assembly of Pd clusters over the C-terminated SiC and amorphous carbon layers, in contrast to the irregular features over Si-terminates SiC surface clearly indicates the role of C on the ordered assembly of the clusters. We believe the C at the surface of the C-terminated SiC and amorphous C films remain unsaturated, forming dangling bonds which act as the nucleation centers for the formation of Pd clusters. Recently a few reports have been published on the assembly of metal clusters over carbon nanotubes without using organic functionalizing agents. Though by controlling the hydrophilicity of CNTs, it is possible to fabricate metal or semiconductor cluster-assemblies over them by proper choice of capping agents over the clusters (11,29), without organic capping agent, metal clusters do not assemble

over the carbon surface. Satishkumar et al. (30) were successful to decorate CNTs by Au, Pt and Ag clusters through nitric acid refluxing. By nitric acid refluxing, they generated acid sites over the nanotube surfaces which acted as nucleation centers. Though by controlling the concentration of the metal ions they could control the surface coverage of metal clusters over the CNT surface, the metal clusters did not form ordered assemblies. In our case, as the whole surfaces of the C-terminated SiC and C-coatings over the microscopic grids were covered with C-sites with dangling bonds, the metal clusters could be assembled in well ordered manner.

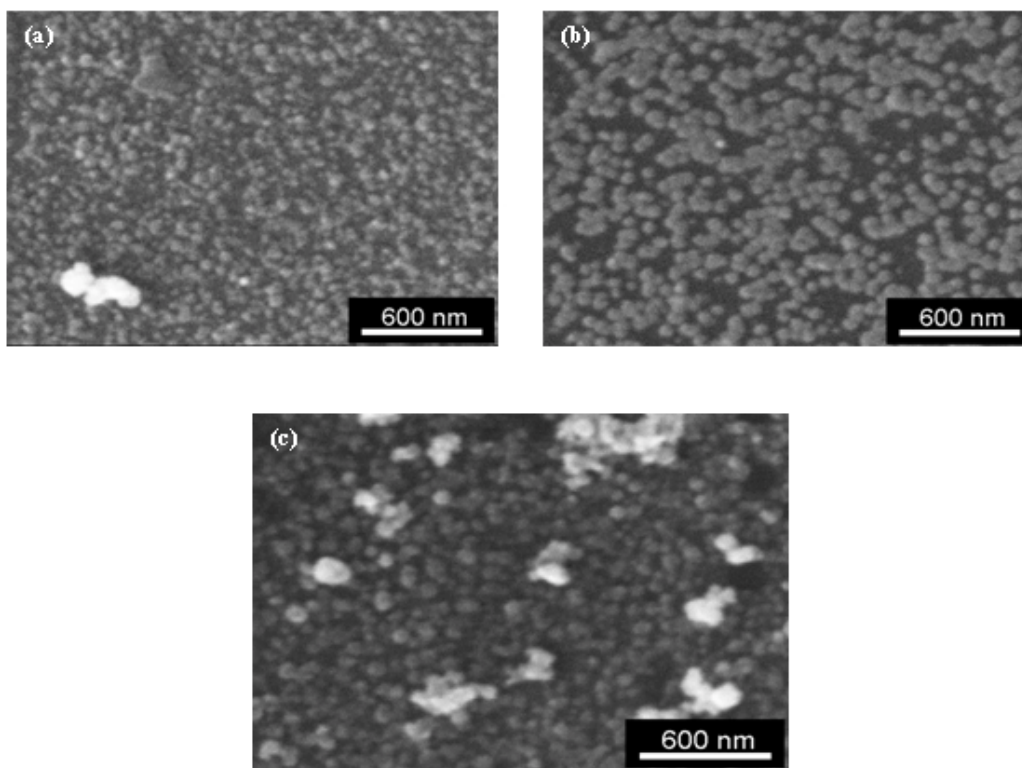


Figure 4 - Typical SEM images of the Pd cluster assemblies formed over amorphous carbon surface for a) 5 min, b) 10 min, and c) 20 min of immersion times.

The use of methanol as the solvent for reducing noble metal ions in is well established (31, 32). On addition of freshly prepared NaBH₄ aqueous solution results the reduction of metal ions following the equation:



The presence of Pd in the clusters could be verified from the EDS spectra of the samples. In figure 5, a typical EDS spectrum of the clusters formed over C-coated Cu grid is shown. While the Cu and C peaks appeared in the spectrum from the C-coated

Cu grids, the Al and O peaks appeared from the Al substrate holder of the microscope. Absence of chlorine peak in the EDS spectrum indicates its complete removal from the sample after washing.

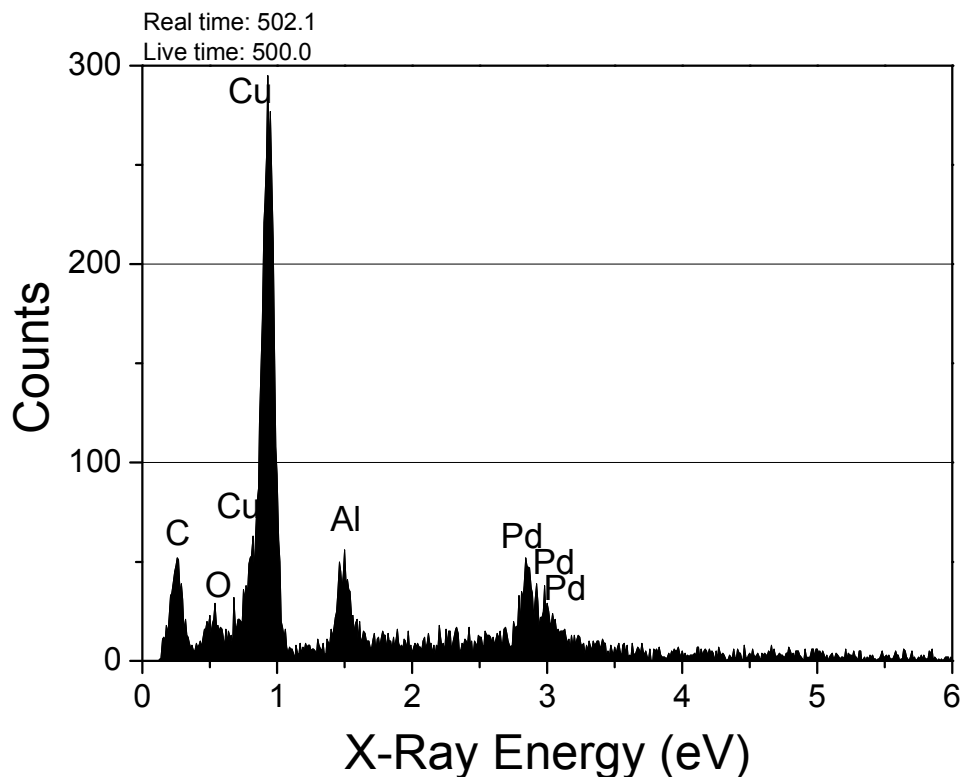


Figure 5 - Typical EDS spectrum of Pd nanoclusters assembled over C substrate. The sample was prepared by immersing the substrate for 20 min in the reaction mixture. The Cu and C peaks appeared from the C-coated Cu grid. The Al and O peaks appeared from the Al sample holder of the microscope.

To observe the formation and characteristic features of the Pd clusters in details, the samples were observed in STM. The C-terminated SiC substrates revealed the formation of nanometric spherical Pd nanoparticles inside the clusters. The average size of the nanoparticles increased from 13 nm to 20 nm on increasing the immersion time from 2 min to 10 min (Figs. 6a-6c). However, for even longer immersion time, the particles did not grow further, but coalesce to form interconnected structures (Fig. 6d).

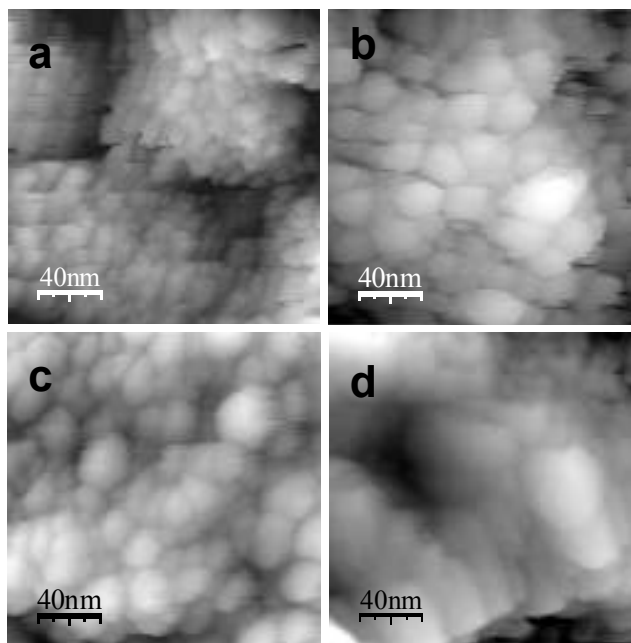


Figure 6 - Typical STM images of the Pd nanoparticles inside of clusters grown over C-terminated SiC substrate for a) 2 min, b) 5 min, c) 10 min, and d) 20 min of immersion in the reaction solution.

For the Pd/C sample, however, the Pd nanoparticles were grown with considerably smaller in size. The average size of the particles varied from 8 nm to 10 nm for the increase of immersion time from 5 min to 20 min (Fig. 7). Moreover, on increasing the immersion time further, the particles did not coalesce much as in case of C-terminated SiC substrates.

We believe the differences in the cluster size between the C-terminated SiC and amorphous carbon substrates might be due to the influence of the dangling bond concentration of the substrates that act as nucleation centers. For amorphous carbon, sp^2 bondings have been proposed to explain the formation of chains and connections between the disordered regions (33), which reduce the tetrahedral sp^3 coordinations. A higher amount of tetrahedral sp^3 dangling bonds in the crystalline SiC are exposed over the C-terminated SiC surface (34-36) which acts as Pd nucleation centers. Presence of sp^3 dangling bonds in higher concentration in the latter case produces dense, compact Pd cluster assemblies as revealed from the SEM images (Figs. 3 and 4) than the earlier. Moreover, this may be a reason for the higher average size of the Pd particles formed over C-terminated SiC substrate than over amorphous carbon for a similar interval of immersion time. For longer time of immersion, while the

nanoparticles formed over amorphous carbon substrate continue to grow without coalescence, the nanoparticles over C-terminated SiC substrates stop growing after about 10 min and coalesce for longer immersion time.

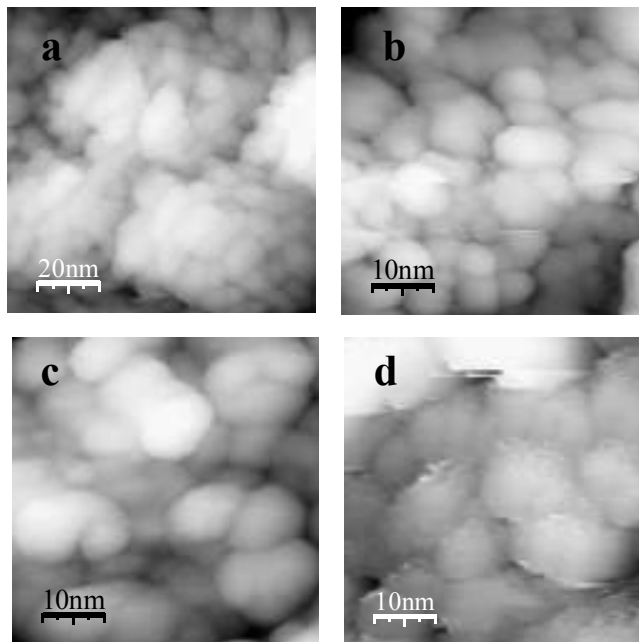


Figure 7 - Typical STM images of the Pd nanoparticles grown over amorphous carbon substrates for a-b) 5 min, c) 10 min, and d) 20 min of immersion in the reaction solution.

Figure 8 shows the representative I-V curves for the Pd particles over carbon and C-terminated SiC substrates. The spectra were recorded putting the tips on isolated Pd particles in both the cases and with the same tip-sample separation. At low voltages, where the tunnel current depends exponentially on the tip-sample separation and surface states density [37], similar values for the tunnel current are observed, and therefore, analogous electronic properties are expected for the Pd nanoparticles in both the samples. At higher voltages, while the Pd nanoparticle over carbon substrate revealed metallic behavior (linear variation of tunneling current), the Pd nanoparticle over SiC revealed non-metallic characteristics. It must be noted that while the carbon substrate we used was electronically of metallic nature, the SiC was a semiconductor with high band gap. It is well known that the tunneling spectra recorded above the supported nanoparticles exhibit chemical states of both the particles and the particle-support (38-41). The linear variation of tunneling current in the case of Pd particles on carbon support indicates that our Pd particles are clean. As all the samples were grown at the same experimental conditions, we believe, the Pd nanoparticles over SiC

substrates are also clean. Therefore, the non-metallic I-V spectrum for the Pd particles over SiC must be due to the interfacial electronic or chemical states between the Pd particle and the substrate, which is not surprising due to semiconducting nature of SiC.

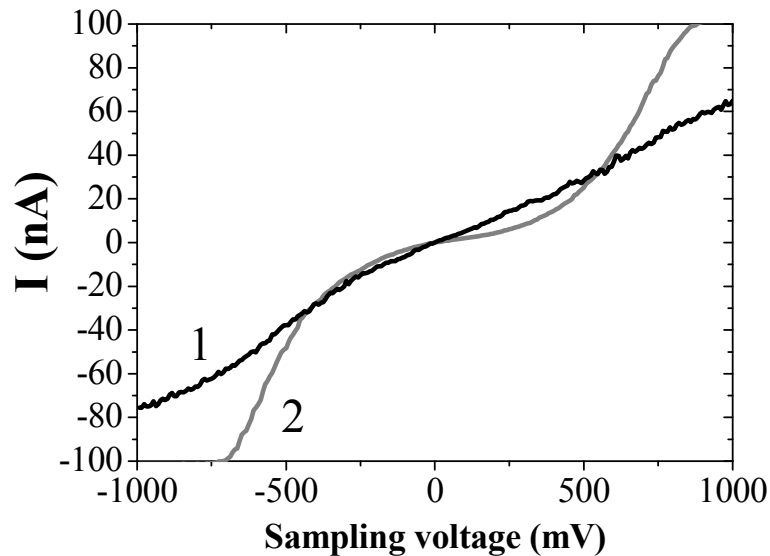


Figure 8 - I-V spectra obtained at 1.2 nA and 50 meV for Pd nanoparticles assembled on (1) amorphous C and (2) C - terminated SiC.

Through atomic resolution STM imaging, we could see that on coalescence, the particles form terraces (Fig. 9). Also both the particles and the terraces are well crystalline. The lattice constant measured ($a = b = 2.8 \text{ \AA}$) from the images agree well with the bulk lattice constant ($a = b = 3.0 \text{ \AA}$) of hexagonal Pd. So, the nanoparticles retain their bulk crystalline structure while being assembled on the substrates.

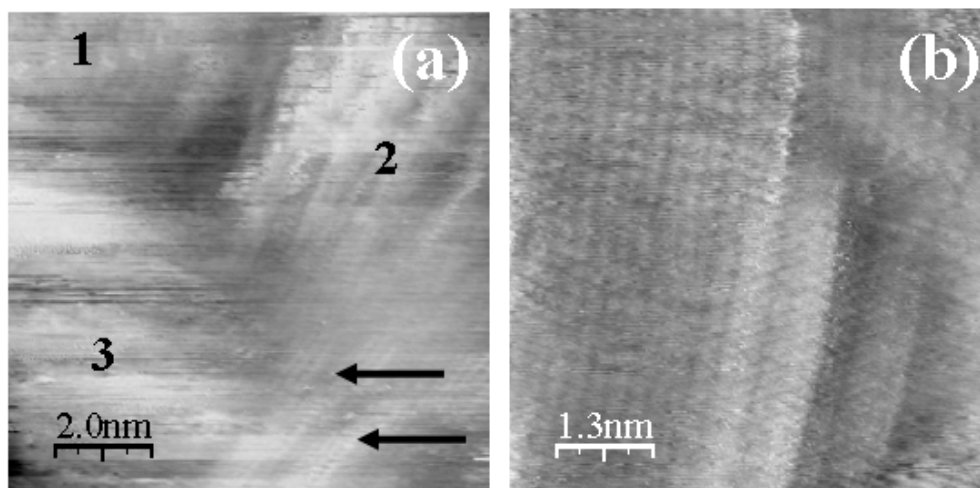


Figure 9 - STM images acquired at 14 mV and 5.6 nA, exhibiting (a) terraces formation during the coalescence of Pd nanoparticles (arrows). (b) Details of the terraces that indicate their hexagonal structure. The labels 1, 2, and 3 in (a) indicate the nanoparticles that participate in the coalescence process.

4. Conclusions

Using a single step chemical technique, ordered-assembly of Pd nanoclusters could be fabricated over C-terminated SiC and amorphous C substrates at room temperature. The size of the metal clusters could be controlled simply by adjusting the immersion time of the substrates in the reaction solution. Sp^3 dangling bonds of carbon on the substrate surfaces are assumed to be responsible for the nucleation and growth of Pd nanoclusters. The assembled Pd clusters are consisting of several nanoparticles and relatively free from contaminations. The Pd clusters are metallic in nature and preserve their bulk crystalline structure while assembled over the electronic substrates. The clusters formed over C-terminated SiC substrates reveal particle-substrate interfacial states in their STS spectra. Using our technique, ordered assembly of other noble metals like Pt, Au, etc. can be prepared over electronic substrates without using any external functionalizing agent.

Acknowledgements

We are grateful to Dr. Valenzuela-Benavides for his help in the STM image acquisition. To Israel Gradilla for his technical help in taking SEM images of the samples. We acknowledge the partial financial helps of CONACyT, VIEP-BUAP, and PAPIIT-UNAM, Mexico, for partial financial helps through Grants No. 46269, 111/EXC/05 and IN113303, respectively.

References

1. Fendler J. H. *Chemistry of Materials* 2001. 13. 3196 p.
2. Whitesides G. M. and Grybowski B. *Science* 2002. 295. 2418 p.
3. Murray C. B. Kagan C. R. and Bawendi M. G. *Annual Review of Materials Science* 2000. 30. 545 p.
4. Suo Z. *International Journals of Solids and Structures* 2000. 37. 367 p.
5. Suo Z. and Lu W. *Journal of Nanoparticle Research* 2000. 2. 333 p.
6. Decher D. *Science* 1997. 277. 1232 p.
7. Kotov N. A. Dekany I. and Fendler J. H. *Journal of Physical Chemistry* 1996. 99. 13065 p.
8. Hammond P. T. *Advanced Material* 2004. 16. 1271 p.
9. Crips M. T. and Kotov N.A. *Nano Letters* 3. 3. 173 p.
10. Caruso F. Caruso R. A. and Möhwald H. *Science* 1998. 282. 1111 p.
11. Correa-Duarte M. A. and Liz-Marzán L. M. *Journal of Material Chemistry* 2006. 16. 22 p.
12. Grisel R. Weststrate K. J. Gluhoi A. and Nieuwenhuys B. E. *Gold Bulletin* 2002. 35. 39 p.
13. Nayral C. Viala E. Fau P. Senocq F. Jumas, J. C. Maisonnat A. and Chaudret B. *Chemistry – A European Journal* 2000. 22. 4082 p.
14. Jitianu A. Altindag Y. Zaharescu M. and Wark M. *Journal of Sol-Gel Science* 2003. 26. 483 p.
15. Jia J. Wang B. Wu A. Cheng G. Li Z. and Dong S. *Analytical Chemistry* 2002. 74. 2271 p.
16. Fendler J. *Chemistry of Materials* 2001. 13. 3196 p.
17. Bethell D. Brust M. Schiffrin D. J. and Kiely C. J. *Electroanalytical Chemistry* 1996. 409. 137 p.
18. Liu S. Zhu T. Hu R. and Liu Z. *Physical Chemistry Chemical Physics* 2002. 4. 6059 p.
19. Snow A. W. Ancona M. G. Kruppa W. Jernigan G. Foos E. and Park D. *Journal of Material Chemistry* 2002. 12. 1222 p.
20. Vidoni O. Neumeier S. Bardou N. Pelouard Jean-Luc and Schmid G. *Journal Cluster Science* 2003. 14. 325 p.

21. Sastry M. Mayya K. S. Patil V. Paranjape D. V. Hegre S. G. *Journal of Physical Chemistry B* 1997. 101. 4954 p.
22. Bardosova M. Tredgold R. H. Ali-Adib Z. *Langmuir* 1995. 11. 1273 p.
23. Mayya K. S. Patil V. Sastry M. *Langmuir* 1997. 13. 2575 p.
24. Pal U. Silva-Gonzalez R. Sanchez-Ramirez J. F. and Diaz-Estrada J. R. *Applied Physics A* 2005. 80. 477 p.
25. Xie Y. H. Samavedam S. B. Bulsara M. Langdo T. A. and Fitzgerald E. A. *Applied Physics Letters* 1997. 71. 3567 p.
26. Kim H. J. Zhao Z. M. and Xie Y. H. *Physical Reviews B* 2003. 68. 205312 p.
27. Mo Y.-W. Kleiner J. Webb M. B. and Lagally M. G., *Surface Science* 1992. 268. 275 p.
28. Blochwitz C. and Tirschler W. *Crystal Research Technology* 2005. 40. 32 p.
29. Haremza J. M. Hann M. A. Krauss T. D. Chen S. and Calcines J. *Nano Letters* 2002. 2. 1253 p.
30. Satishkumar B. C. Vogl E. M. Govindaraj A. and Rao C. N. R. *Journal of Physics D: Applied Physics* 1995. 29. 3173 p.
31. Sánchez Ramírez J. F. Pal U. *Journal of New Material for Electrochemical System* 2005. 8. 127 p.
32. Esparza R. Ascencio J. A. Rosas G. Campos R. Sanchez Ramirez J. F. and Pal U. *Journal of Nanoscience and Nanotechnology* 2005. 5. 641 p.
33. Walkers J. K. Gilkes K. W. R. Wicks J. D. and Newport R. J. *Journal of Physics: Condensed Matter* 1997. 9. L457 p.
34. Pensl G. Morkoc H. Monemar B. Janzen E. *Silicon Carbide III-Nitrides, and related Materials* Materials Science Forum, Trans Tech., Switzerland 1998. 264-268 p.
35. Deryck V. Soukiassian P. G. Amy F. Chabal Y. J. D'angelo M. D. Enriquez H. B. and Silly M. G. *Nature Materials* 2003. 2. 253 p.
36. Cantin J. L. Von Bardeleben H. J. Shishkin Y. Ke Y. Devaty, R. P. and Choyke W. J. *Physical Review Letters* 2004. 92. 015502 p.
37. Stroscio J. A. and Kaiser W. J. *Scanning Tunneling Microscopy* Academic Press Inc., USA 1993.
38. Bäumer M. Freund H-J. *Progress in Surface Science* 1999. 61. 127 p.
39. Bifone A. Casalis L. Riva R. *Physical Review B* 1995. 51. 11043 p

40. Radojkovic P. Schwartzkopff M. Enachescu M. Stefanov E. Hartmann E. Koch F. *Journal of Vacuum Science and Technology B* 1996. 14.1229 p.
41. Szökó J. Berkó A. *Vacuum* 2003. 71. 193 p.